

The Effect of Casting Mold Material on Microstructure of Al-Si Alloys

Tomas Vlach (0000-0003-2326-4183), Jaromir Cais (0000-0002-1726-5326)

Faculty of Mechanical Engineering, J. E. Purkyne University in Usti nad Labem. Pasteurova 3334/7, 400 01 Usti nad Labem. Czech Republic. E-mail: tomas.vlach@ujep.cz

This article deals with the influence of the mold material on the segregation process in selected Al-Si alloys. Three types of Al-Si alloys were chosen in order to compare the segregation process while congelating. AlSi7Mg0.3, AlSi7Cu4 and AlSi10.5Cu1.2Mn0.8Ni1.2Pb0.5 alloys were cast by gravity casting in a metal and sand molds. Macroscopic and microscopic analysis of the internal structure of each of the alloys was also studied. The chemical composition within the lower, middle and upper parts of the casts were observe by using scanning electron microscope. All samples were subjected to the Vickers microhardness measurement of a solid solution of $\alpha(\text{Al})$. The microhardness measurement was performed to verify the constancy of the mechanical properties of the solid solution $\alpha(\text{Al})$ under different solidification conditions. The distance between the secondary axes of the dendrites DAS (Dendrite Arm Spacing) was used to evaluate the level of segregation.

Keywords: segregation, heterogeneity, aluminium alloys, microstructure, DAS, microhardness

1 Introduction

Aluminum is one of the most common elements on earth and is mainly used in alloys in combination with various elements [1]. Mechanical properties can be improve by adding alloying elements [2]. Aluminum alloys are one of the most widely used metal materials [3]. According to the processing technology, aluminum alloys can be divided into alloys suitable for forming and for casting [1].

Al-Si alloys represent the largest part of casting materials [2]. They are mostly casted using gravity casting. Gravity casting is the processes, where the mold is filled with melt due to gravity [4,5]. It can be cast into sand or metal molds. Gravity casting of light alloys is mainly used in the automotive industry, such as cylinder heads, wheel discs etc. [6,7].

On the other hand the gravity casting can cause a number of undesirable phenomena (e.g., segregation). Aluminum alloys with a higher number of alloying elements are prone to segregation. Segregation affects the mechanical, chemical and physical properties of the alloy [8]. The cause of segregation is the gradual solidification of the grain during the gradual transformation of the solid phase [9,10]. The degree of segregation depends, among other things, on the cooling rate and is related to the distance from the main axes

of the dendritic cells. In the sand form, the melt will solidify more slowly, the distance between the main axes of the dendritic cells will be longer.

Metalic form helps faster solidification resulting into the smaller distance between the main axes of the dendritic cells, and a fine-grained structure is formed. A greater distance between the main axes of the dendritic cells facilitates segregation during the lower cooling rate. The cooling process is related to heat removal and is significantly affected by the material of the mold [8]. Segregation in the alloy cannot be prevented, but it can be suppressed by homogenization annealing [11].

2 Materials and methods

Three alloys were used in order to conduct this research. AlSi7Mg0.3 alloy, designated according to European standards as EN AC-42100. Is usually used for casting. Due to the possibility of its hardening, it is widely used in the automotive and aviation industries [12,13]. This alloy was assumed to have the lowest level of segregation due to the low content of alloying elements. Mg_2Si , Al_5FeSi type phases are assumet to be present within this alloy microstructure. The chemical composition of the this alloy according to the standard is presented in Tab 1 below.

Tab. 1 Chemical composition of AlSi7Mg0.3 [12]

Chemical el.	Al	Si	Mg	Ti	Fe	Mn	Zn	Cu
wt [%]	91.3-93.3	6.5-7.5	0,25-0.45	0-0.25	0-0.19	0-0.1	0-0.07	0-0.05

Tab. 2 Measured chemical composition of AlSi7Mg0.3

Chemical el.	Al	Si	Mg	Ti	Fe	Mn	Zn	Cu
wt [%]	base	6.9	0.31	0.25	0.17	0.1	0.06	0.03

Tab. 3 Chemical composition of AlSi10.5Cu1.2Mn0.8Ni1.2Pb0.5 [14]

Chemical el.	Al	Si	Cu	Mn	Ni	Pb
wt [%]	85.8	10.5	1.2	0.8	1.2	0.5

Tab. 4 Measured chemical composition of AlSi10.5Cu1.2Mn0.8Ni1.2Pb0.5

Chemical el.	Al	Si	Cu	Mn	Ni	Pb
wt [%]	base	10.6	1.1	0.9	1.3	0.4

Tab. 5 Chemical composition of AlSi7Cu4 [15]

Chemical el.	Al	Si	Mn	Cu	Pb	Fe	Zn	Mg
wt [%]	≥80	6.5-8.0	≤0.65	3.0-4.0	≤0.15	≤0.8	≤0.65	0.3-0.6

Tab. 6 Measured chemical composition of AlSi7Cu4

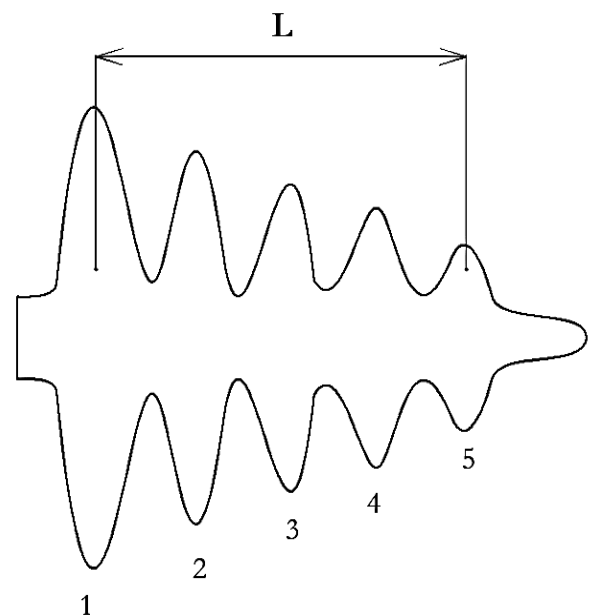
Chemical el.	Al	Si	Mn	Cu	Pb	Fe	Zn	Mg
wt [%]	base	6.8	0.5	4.0	0.04	0.55	0.25	0.3

The second observe alloy was AlSi10.5Cu1.2Mn0.8Ni1.2Pb0.5 without a standardized designation. The AlSi10.5Cu1.2Mn0.8Ni1.2Pb0.5 alloy was developed as a replacement for the AlSi7Mg0.3 alloy and was granted European patent EP306352. This alloy contains a large number of alloying elements, there is an assumption of the highest degree of segregation compared to other alloys. Al_3FeSi , Al_3Ni or Al_2Cu type phases will probably form in the alloy. The chemical composition of the given alloy is presented in Tab 2 below [14].

Another alloy was the AlSi7Cu4 alloy, referred as EN AC-46300 according to the standards [15]. It is an alloy intended for casting and can be also hardened. It is used where high strength and stiffness are required. It is used in automotive industry, aviation industry etc. For this alloy, the assumption of a higher degree of segregation than for the AlSi7Mg0.3 alloy, but at the same time lower than for the AlSi10.5Cu1.2Mn0.8Ni1.2Pb0.5 alloy. There will likely be Al_2Cu and Al_3FeSi type phases can occur within the alloy microstructure [16]. The chemical composition of the given alloy according to the standard is presented in Tab 3 below.

The most common method for determining the dendritic structure is the DAS (Dendrite Arm Spacing) method. Dendrite dispersion, which is the distance between the secondary axes of the dendrites (see Fig. 1). The distance is usually between 10 and 150 μm . These values were metallographically determined

using a confocal microscope. DAS values depends on the rate of cooling of the alloy in the solidification interval [1].



$$DAS = L / (n - 1) [\mu m]$$

n ... number of secondary axes

L ... distance between secondary axes

Fig. 1 DAS measurement scheme

2.1 Prepared samples

Melting was conducted in graphite crucibles in an electric resistance furnace. The casting temperature was $730\text{ }^{\circ}\text{C} \pm 5^{\circ}\text{C}$. Before casting into molds, the melt was refined using ECOSAL refining salt. Each alloy was cast in a sand and metal molds. The molds were preheated at temperature of $200\text{ }^{\circ}\text{C}$ in order to remove possible humidity. Samples were cut out from three places of the casts. The scheme of sampling locations is denoted in Fig. 2 below.

A total of 18 samples were prepared. Labeling of the samples, type of alloy, material of the mold and place of sampling is presented in Tab 4.

Tab. 4 Materials used for sample preparation

Sample	Substrate	Casting mold material	Cast sampling area
AK1	AlSi7Mg0.3	Metal	bottom part of the cast
AK2			middle part of the cast
AK3			top part of cast
AP1		Sand	bottom part of the cast
AP2			middle part of the cast
AP3			top part of cast
BK1	AlSi10.5Cu1.2Mn0.8Ni1.2Pb0.5	Metal	bottom part of the cast
BK2			middle part of the cast
BK3			top part of cast
BP1		Sand	bottom part of the cast
BP2			middle part of the cast
BP3			top part of cast
CK1	AlSi7Cu4	Metal	bottom part of the cast
CK2			middle part of the cast
CK3			top part of cast
CP1		Sand	bottom part of the cast
CP2			middle part of the cast
CP3			top part of cast

3 Results

3.1 Confocal microscopy

A Laser Confocal Microscope Olympus OLS 3100 was used to examine the microstructure of all samples. Due this analysis, it is possible to observe a solid solution of aluminum α and eutectic, which is excluded along the borders of dendritic cells, in all images (see



a)



b)

Fig. 3 Microstructure of the AlSi7Mg0.3 alloy – bottom part of the cast,
a) metal mold b) sand mold

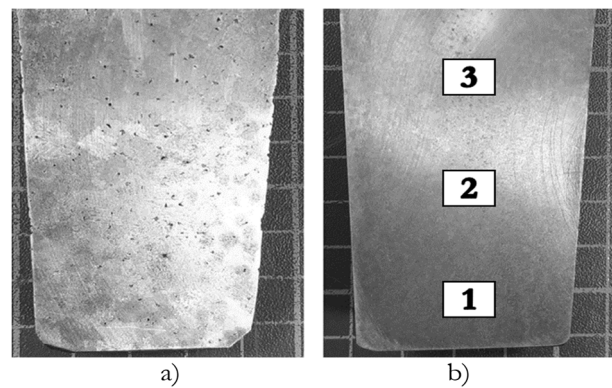


Fig. 2 Macrostructure of
AlSi10.5Cu1.2Mn0.8Ni1.2Pb0.5 alloy
a) sand mold b) metal mold

Fig. 3-5). The eutectic is formed by a solid solution of α and silicon particles. In the images below, we can observe The differences in the size of the dendritic cells in the samples cut out from the upper part of the casting casting can be observed. In metal mold castings, the size of the dendrites is significantly smaller than in sand mold castings. This is due to the faster cooling rate – the metal mold dissipates heat better.

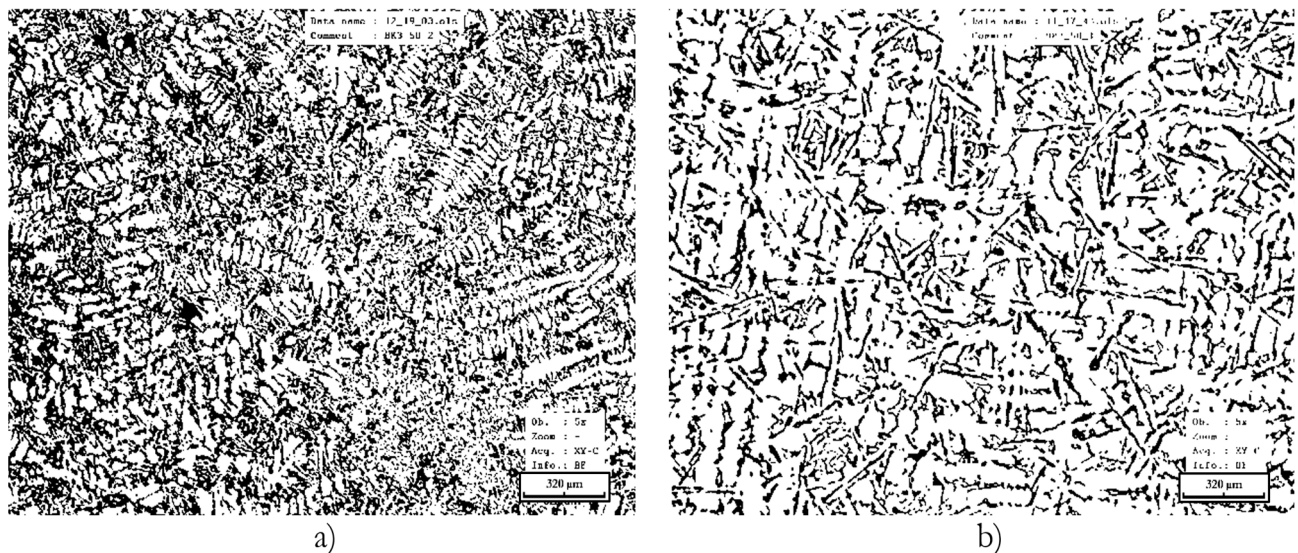


Fig. 4 Microstructure of the $AlSi10.5Cu1.2Mn0.8Ni1.2Pb0.5$ alloy – bottom part of the cast, a) metal mold b) sand mold

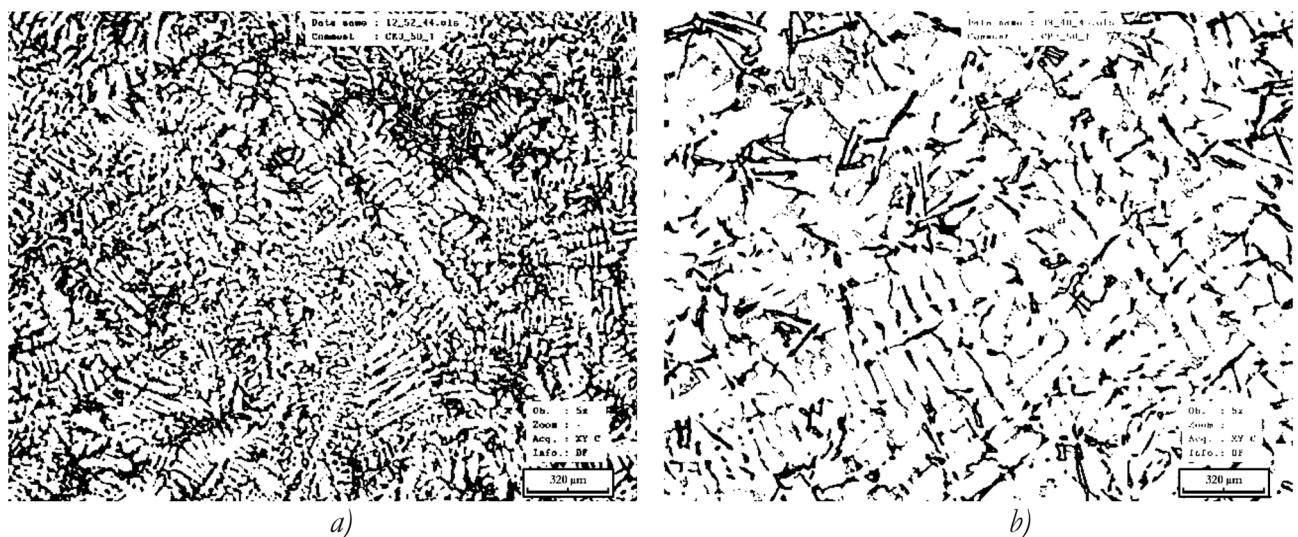


Fig. 5 Microstructure of the $AlSi7Cu4$ alloy – bottom part of the cast, a) metal mold b) sand mold

3.2 Scanning electron microscopy

The samples were examined using a Scanning Electron Microscope Tescan VEGA 3 with EDX detector Bruker X-Flash Nano. The analysis was performed for sampling area 2 (middle part of the cast) of each alloy. Using confocal microscopy, these samples were selected to identify intermetallic phases and elemental distributions.

Figures 6-8 show elemental maps from three samples – AK2, BK2 and CK3. Figure 6 shows the elemental map of sample AK2 from $AlSi7Mg0.3$ alloy. In addition, the intermetallic phase Al_5FeSi , precipitated in the shape of a needle, was captured in the investigated area.

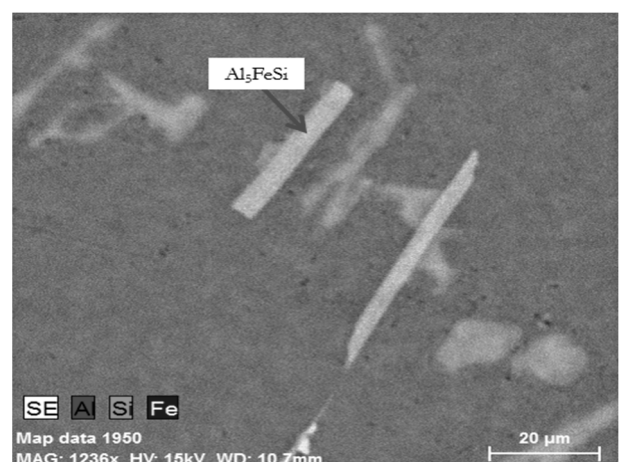


Fig. 6 Element map of sample AK2

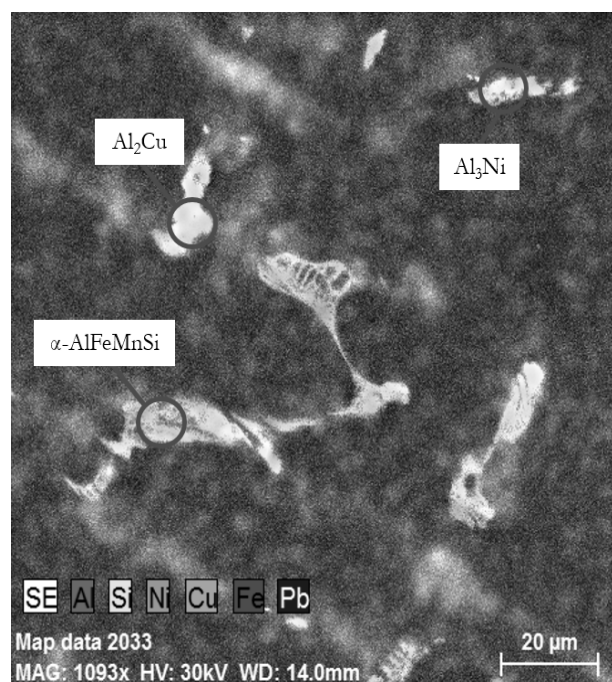


Fig. 7 Element map of sample BK2

Figure 7 shows the elemental map of the selected area from the AlSi10.5Cu1.2Mn0.8Ni1.2Pb0.5 alloy from the BK2 sample. In addition, the following phases were also detected in the investigated alloy: α -AlFeMnSi, Al_3Ni and Al_2Cu . As can be seen in Fig. 7, the α -AlFeMnSi phase was excluded in the form of a skeletal structure - they are so called „Chinese script“.

The elemental map of the selected area from the AlSi7Cu4 alloy are presented on Figure 8 (from the BK2 sample). The figure also represents the Al_5FeSi and Al_2Cu phases. The second Al_2Cu phase were excluded along the grain boundaries.

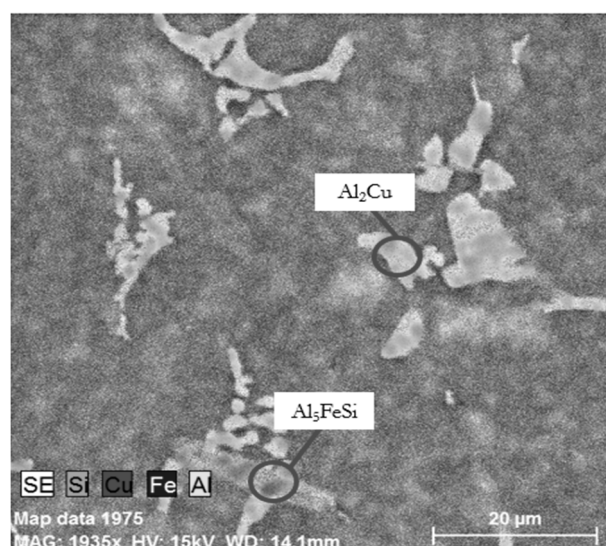
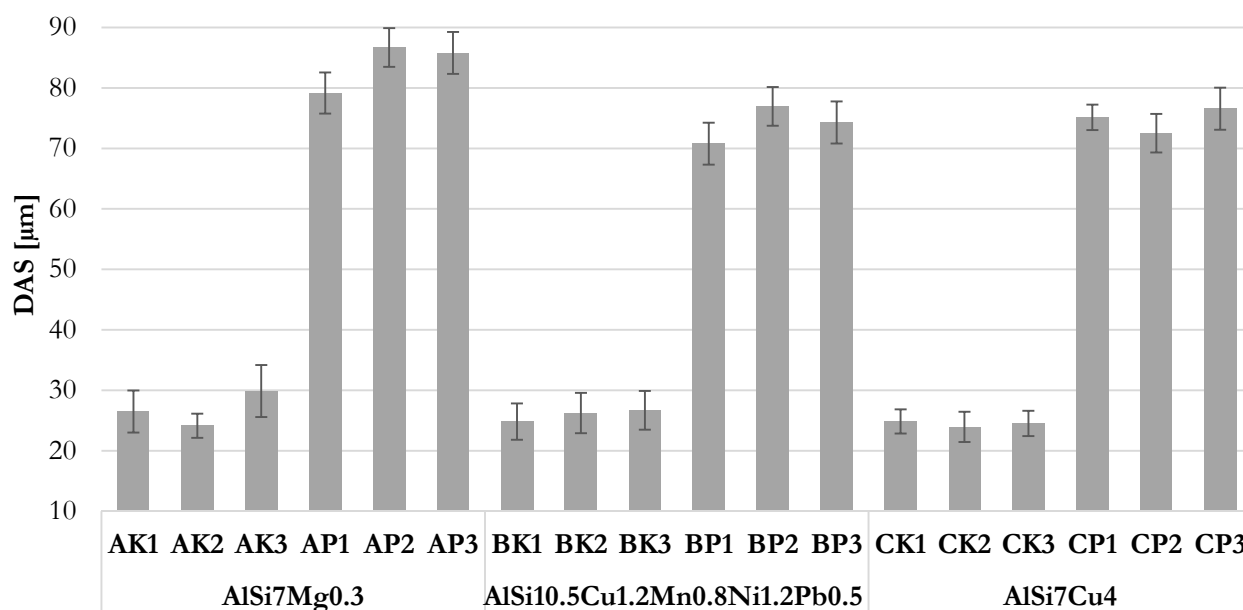


Fig. 8 Element map of sample CK2

3.3 Dendrite arm spacing

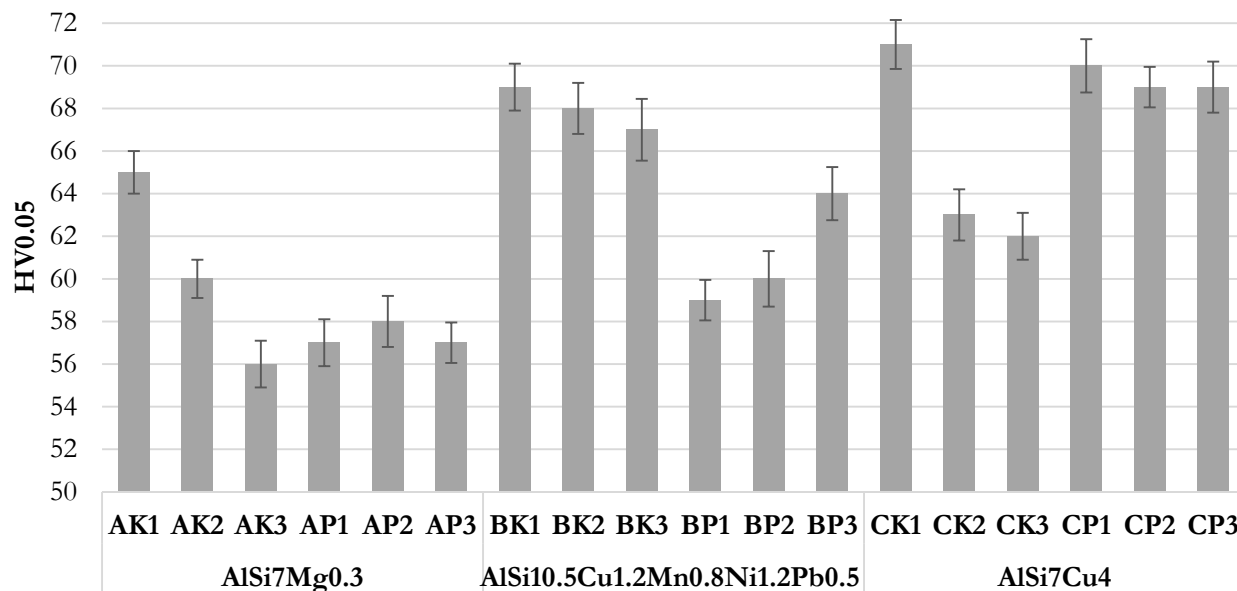
The Graph 1 shows the average values from the measured values of the distances of the secondary axes of the dendrites for all samples from both sand and metal mold castings. The values for the sand mold samples are approximately three times higher than the values for the metal mold samples. The different values were caused by the different cooling gradient between the metal and sand molds. The largest size of dendrites was acquired by the AlSi7Mg0.3 alloy casting cast in a sand mold. The AlSi10.5Cu1.2Mn0.8Ni1.2Pb0.5 and AlSi7Cu4 alloy samples that were cast in a sand mold had approximately the same grain size. This phenomenon can be observed for the grain size of castings from metal molds.



Graph 1 Dendrite arm spacing of prepared samples

3.4 Microhardness

All of the samples were subjected to microhardness analysis. 10 measurements were conducted on each sample via SHIMADZU HMV Micro Hardness Tester. The average microhardness values of the aluminum solid solution of all samples was presented in the Graph 2 below.



Graph 2 Microhardness of solid solution a prepared samples

4 Conclusion

Casting into different casting molds causes different solidification conditions in dependants of the mold material. A metal mold has a higher cooling gradient than a sand mold. This significantly affected the process of segregation. The different cooling rate was significantly reflected in both macrostructure and microstructure.

Results indicate that the casts of the metal mold acquire higher values of the microhardness of the solid solution α in comparison with the sand mold casts. AlSi7Mg0.3 alloy castings from a metal mold reveal in average 5 % higher values of solid solution microhardness α compared to sand mold casts. For the AlSi10.5Cu1.2Mn0.8Ni1.2Pb0.5 alloy microhardness difference increases up to 12 %. For the AlSi7Cu4 alloy, the increase is in average 6 %.

Significantly larger dendritic cells can be observed within sand mold casts in comparison with metal mold casts. Sand mold AlSi7Mg0.3 alloy casts reveal in average 68 % larger dendrite size than metal mold casts. For the AlSi10.5Cu1.2Mn0.8Ni1.2Pb0.5 alloy the grain size increased by 65 %. For the AlSi7Cu4

The highest microhardness values of aluminum solid solution for each alloy are shown by castings from a metal mold. Microhardness decreases with increasing distance from the bottom of the casting. For castings from sand forms, significant differences in microhardness values cannot be observed. The highest microhardness values was revealed within the AlSi7Cu4 alloy, in both metal and sand mold castings.

alloy grain size increases 67 % on average.

Al₅FeSi intermetallic phases were identified in the AlSi7Mg0.3 alloy. Al₅FeSi, Al₃Ni and Al₂Cu intermetallic phases were identified in the AlSi10.5Cu1.2Mn0.8Ni1.2Pb0.5 alloy, which contained the largest amount of alloying elements. Intermetallic phases Al₂Cu and Al₅FeSi were identified within AlSi7Cu4 alloy.

The aim of the research was to compare the character of the microstructures of various AlSi-type hypoeutectic alloys depending on the material of the casting mold used. It was found and confirmed that the newly developed AlSi10.5Cu1.2Mn0.8Ni1.2Pb0.5 alloy has the same grain refinement effect as AlSi7Mg0.3 alloy and AlSi7Cu4 alloy when using metal molds.

Acknowledgment

This research was supported by the internal UJEP Grant Agency (UJEP-SGS-2022-48-004-2).

References

- [1] ROUČKA J., (2004). *Metallurgie neželezných slitin*, CERM s.r.o., Brno, ISBN 80-214-2790-6
- [2] DURAI, K., SUNDAR, S., SUNDARLINGAM, P.,

- HARSHAVARDHANA, N. (2021). Optimization of highspeed machining cutting parameters for end milling of AlSi7Cu4 using Taguchi based technique of order preference similarity to the ideal solution, *Materials Today: Proceedings*, Vol. 47, No. 19, pp. 6799-6804, ISSN 2214-7853.
- [3] MICHNA, Š., MICHNOVÁ L. (2014). *Neželezné kovy*, PrintPoint s.r.o., Praha, ISBN 978-80-260-7132-7
- [4] TAYLOR, J.A. (2012). Iron-containing intermetallic phase in Al-Si based casting alloys. In: *Procedia Materials Science*. Vol 1, pp. 19-33.
- [5] DINNIS, C. M. et al., (2005). As-cast morphology of iron-intermetallics in Al-Si foundry alloys, *Scripta Materialia* 53 (8), pp. 955-958.
- [6] TILLOVÁ, E., CHALUPOVÁ, M. (2009). *Štruktúrna analýza zliatin Al-Si*. EDIS Žilina. 191 s. ISBN 978-80-554-0088-4
- [7] BOLIBRUCHOVÁ, D., BRŮNA, M. (2017). Impact of the Elements Affecting the Negative Iron Based Phases Morphology in Aluminium Alloys – Summary. Results In: *Manufacturing Technology*. ISSN 1213-2489. Vol. 17, No. 5, p. 675-679
- [8] WEISS, V., SVOBODOVÁ, J. (2015). The Use of Colour Metallography and EDS for Identification of Chemical Heterogeneity of Selected Aluminium Alloys Copper and Zinc Alloyed. *Manufacturing Technology*, vol. 15, iss. 6, p. 1048-1053.
- [9] WEISS, V., (2012). Hodnocení vlivu teploty a doby homogenizačního žíhání slitiny AlCu4MgMn z hlediska mikrostruktury, obrazové analýzy a metody EDX. *Strojírenská technologie*, vol. 17, iss. 5-6, p. 348-355.
- [10] WEISS, V., STŘIHAVKOVÁ, E. (2011). Optimalizace homogenizačního žíhání slitiny AlCu4MgMn. *Strojírenská technologie*, vol. 16, iss. 5, p. 42-49.
- [11] WEISS, V. (2016). Research of the Chemical Heterogeneity during Crystallization for AlCu4MgMn Alloy and the Possibility of its Elimination. *Manufacturing Technology*, 2016, vol. 16, iss. 1, p. 289-294.
- [12] *EN AC-42100 (AlSi7Mg0.3) Cast Aluminum*. (2022). MakeItFrom.com: Material Properties Database
- [13] AlSi7Mg0.3 – *Aluminium Silicium Alloy*. (2022). Jura-Guss Beilngries | Aluminium Gießerei, Sandguss, Kokillenguss, Modellbau [online]
- [14] MICHNA, Š. CAIS, J. (2016), Hliníková slitina, zejména pro výrobu odlitků segmentů forem pro lisování pneumatik, a způsob tepelného zpracování odlitků segmentů forem. UJEP, Usti nad Labem, Česká republika. *Patentový spis CZ 306352 B6*. 2.11.2016, EP306352
- [15] *EN AC-46300 (AlSi7Cu4)* (2022) European Steel and Alloy Grades / Numbers, SteelNumber, steelnumber.com [online].
- [16] LM21.[online]. [Cit. 19.3. 2022]. Dostupné z: <http://www.nortal.co.uk/LM21/>